

**1. EMISSION OF HIGH ENERGY  
PROTONS AND PIONS IN HEAVY ION  
COLLISIONS IN A NON-EQUILIBRIUM  
HYDRODYNAMIC APPROACH**

**2. ON SPECTRA OF PROTONS IN HEAVY ION  
COLLISIONS  $^{12}\text{C}+^9\text{Be}$  AT ENERGIES OF 0.3-  
2.0 GEV PER NUCLEON IN A  
HYDRODYNAMIC APPROACH**

***A.T.D'yachenko<sup>1,2</sup>, I.A. Mitropolsky<sup>2</sup>***

*<sup>1</sup>Emperor Alexander I Petersburg State Transport  
University;*

*<sup>2</sup>NRC "Kurchatov Institute" B.P. Konstantinov  
Petersburg Nuclear Physics Institute*

*A hydrodynamic approach with a nonequilibrium equation of state is developed to describe the emission of protons and pions formed in collisions of heavy ions of intermediate energies, an amendment for the microcanonical distribution is taken into account, and the contribution of the fragmentation process is included. Experimental data of ITEP(Moscow) on collisions of  $^{12}\text{C}$  nuclei with a beryllium target at energies of 0.3-2 GeV per nucleon for carbon nuclei with proton emission are considered. It is shown that these data can be described within a hydrodynamic model for high-energy cumulative region of the proton spectrum, taking into account the contribution from ion fragmentation for the soft spectral region within the framework of the statistical fragmentation model. The calculated double differential cross sections for pion emission at these energies agree with the available experimental data.*

Ядро-снаряд

Спектаторы снаряда

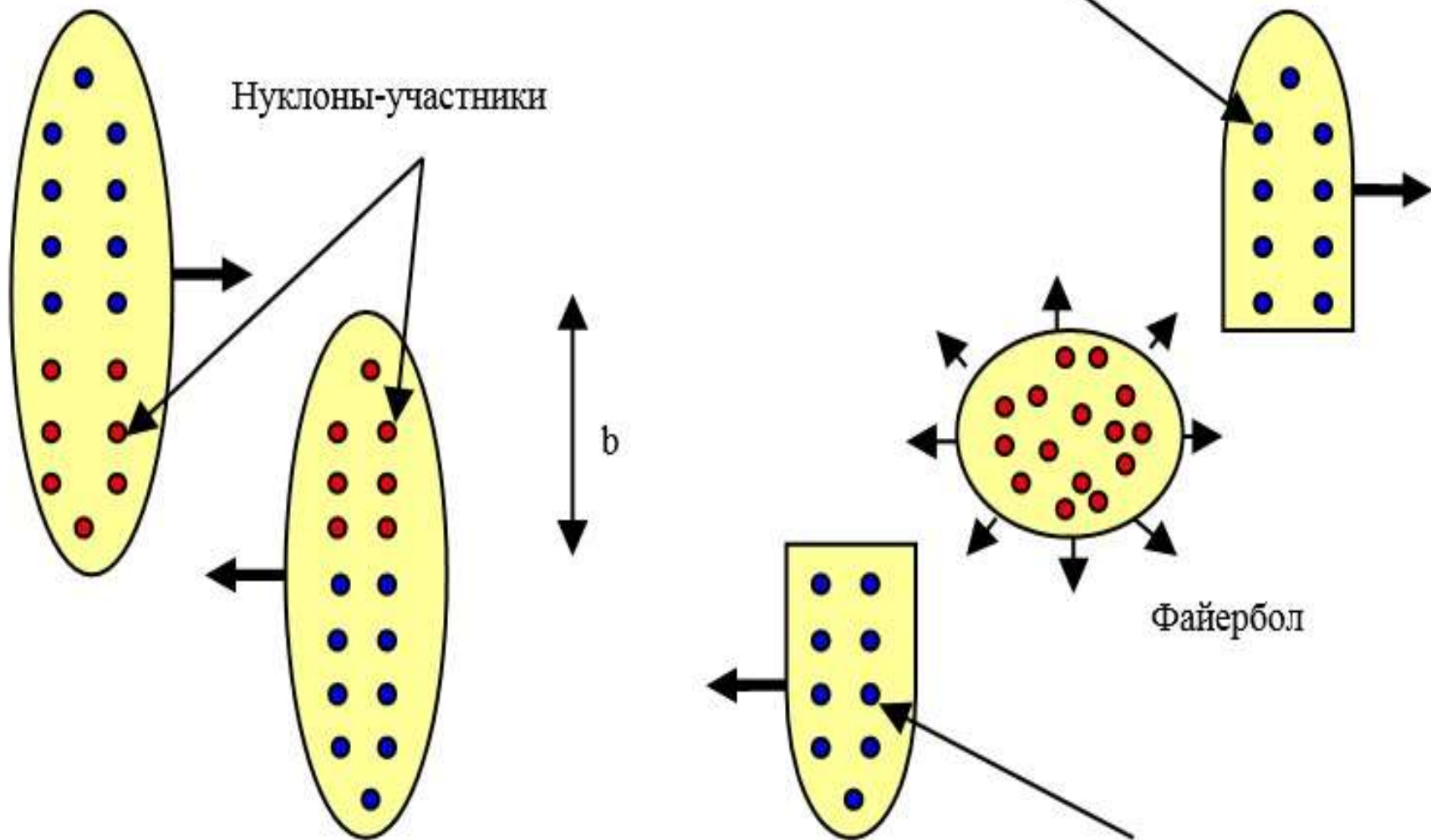
Нуклоны-участники

b

Файербол

Ядро-мишень

Спектаторы мишени



# 1. FEATURES OF NON-EQUALIBRIUM HYDRODYNAMIC APPROACH

- To describe the collisions of heavy ions we use the non-equilibrium hydrodynamic approach, in which the kinetic equation for the nucleon distribution function  $f(\mathbf{r}, \mathbf{p}, t)$  is solved jointly with the equations of hydrodynamics, which are essentially local laws of conservation of mass, momentum and energy.  $\int \frac{d^3 \vec{p}}{(2\pi\hbar)^3} 1, \vec{p}, p^2$

$$\frac{df}{dt} = \frac{f_0 - f}{\tau}, \quad (1)$$

- where  $f_0(\mathbf{r}, \mathbf{p}, t)$  is the locally equilibrium distribution function and
- '  $\tau$  is the relaxation time

$$W(\rho) = \alpha\rho + \beta\rho^\chi, \quad (2)$$

- The self-consistent potential appearing in the interaction term is specified in just the same way as this is done in the case of density-dependent forces belonging to the Skyrme type

- $\rho = \int \frac{f d^3 \vec{p}}{(2\pi\hbar)^3} \quad \tau = \lambda / v_T \quad W(\rho) = \alpha\rho + \beta\rho^\gamma,$
- $f(\vec{r}, \vec{p}, t) = f_1 \cdot q + f_0 \cdot (1 - q)$

(3)

- $P_{kin}^{\parallel} = P_{(kin)11} = 2(\varepsilon_1 + I_1)q + \frac{2}{3}(\varepsilon + I)(1 - q) \quad \varepsilon_1 = \frac{\hbar^2}{10m} \left( \frac{3}{2} \pi^2 \rho_0 \right)^{2/3} \frac{\rho^3}{\rho_0^2}$

- $P_{kin}^{\perp} = P_{(kin)22} = P_{(kin)33} = 2\varepsilon_2 + \frac{2}{3}(\varepsilon + I)(1 - q) \quad \varepsilon_2 = \frac{\hbar^2}{10m} \left( \frac{3}{2} \pi^2 \rho_0 \right)^{2/3} \rho$

- $\varepsilon = \frac{3}{10} \frac{\hbar^2}{m} \left( \frac{3}{2} \pi^2 \rho \right)^{2/3} \cdot \rho \quad I = \int \frac{p^2}{2m} \delta f \frac{d^3 \vec{p}}{(2\pi\hbar)^3} \quad I_1 = \int \frac{p^2}{2m} \delta f_1 \frac{d^3 \vec{p}}{(2\pi\hbar)^3}$

- $P_{ij} = P_{(kin)ij} + P_{int} \delta_{ij} \quad e = \varepsilon + I + e_{int} \quad e_{int} = \int_0^{\rho} W(\rho) d\rho \quad P_{int} = \rho^2 \frac{d(e_{int} / \rho)}{d\rho}$
- $\frac{\partial}{\partial t} ((\varepsilon_1 - \varepsilon_2 + I_1)q) + \frac{\partial}{\partial x_1} (v_1 (3\varepsilon_1 - \varepsilon_2 + 3I_1)q) + \sum_{i=2,3} \frac{\partial}{\partial x_i} (v_i (\varepsilon_1 - \varepsilon_2 + I_1)q) +$

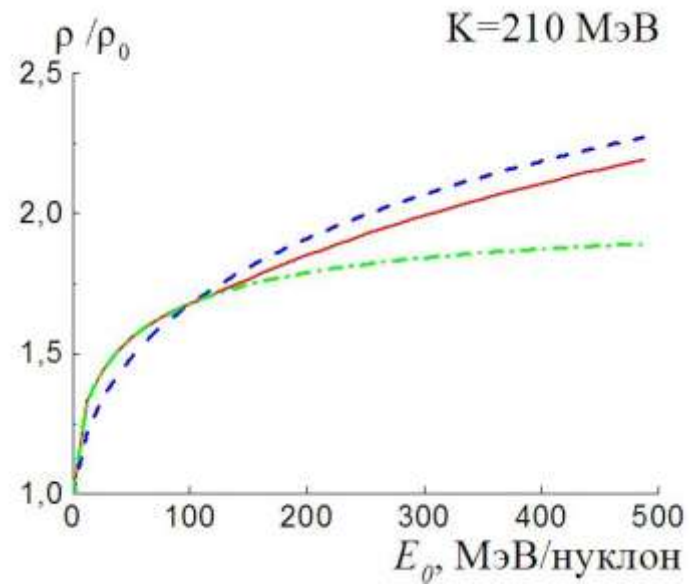
- $\rho v_1 \frac{\partial W}{\partial x_1} - \sum_{i=2,3} \frac{\rho v_i}{2} \frac{\partial W}{\partial x_i} = - \frac{(\varepsilon_1 - \varepsilon_2 + I_1)q}{\tau}$

$$p_1^2 - (p_2^2 + p_3^2) / 2$$

(4)

## 2.THE HYDRODYNAMIC STAGE

- After selecting the region of the local heating, hot spot - the overlap region of the colliding nuclei, we analyze the stages of compression, expansion and freeze-out of matter during the collision of heavy ions. At the compression stage, a collisionless shock wave with a changing front is formed. At the expansion stage, when the shock wave reaches the boundaries of hot spot, the initially compressed system is expanded, we describe it in the relaxation approximation taking into account the nuclear viscosity. As the relaxation time we take  $\tau = \lambda / v_T$  where  $\lambda = 1/\sigma\rho$  is the mean free path,  $\sigma \approx 40\text{mb}$  is the total nucleon-nucleon cross section,  $\rho$  is the nucleon density, and
- $v_T$  is the average velocity of the thermal motion of the nucleons. At the freeze-out stage, when the system reaches a critical density also called the freeze-out density, the system does not "hold itself" and the secondary particles are formed.



- Fig. 1. Dependence on the collision energy of the maximum compression ratio
- $\rho/\rho_0$  achieved in the central collision of nuclei for the case of the relaxation factor
- $q$  (solid line) calculated by us, for the case when the factor  $q=0$
- (dashed line), and for the case when  $q=1$  (a dashed-dot line)

### 3. STATISTICAL FRAGMENTATION MECHANISM

- To describe the soft part of the spectrum of emitted protons, one can use the statistical model of fragmentation of colliding heavy ions proposed by Feshbach, Huang, and Goldhaber . According to this model, the probability of the escape of fragments from a compound nucleus is proportional to  $\exp\left(-\frac{p^2}{2\sigma_K^2}\right)$

- where  $p$  is the momentum of the fragment in the rest frame of the nucleus, and the variance

- $\sigma_K^2 = \sigma_0^2 \frac{K(A-K)}{A-1}$     1)     $\sigma_0^2 = \frac{\langle p^2 \rangle}{3} = \frac{1}{3} \frac{3}{5} p_F^2$ ,  $p_F = \sqrt{2m(E^* - 3/2T)}$     2)     $\sigma_0^2 = mT$

- As a result, we find the contribution we need to the cross section for protons during fragmentation ( $b$  is the impact parameter)

$$E \frac{d^2\sigma}{p^2 dp d\Omega} = \frac{2\pi}{(2\pi\hbar)^3} \int b db \int C d\mathbf{r} r \gamma(E - \vec{p}\vec{v}) \exp\left(-\frac{(\mathbf{p} - \mathbf{p}_0)^2}{2\sigma_0^2}\right)$$



## 4. A COMPARISON WITH EXPERIMENTAL DATA

- As a result, the double differential cross-section of proton emission has the form (where  $b$  is the impact parameter,  $\hbar$  is a Planck constant,  $\vec{r}$  is the radius vector):

$$E \frac{d^2\sigma}{p^2 dp d\Omega} = \frac{2\pi}{(2\pi\hbar)^3} \int G(b) b db d\vec{r} \gamma(E - \vec{p}\vec{v}) f(\vec{r}, \vec{p}, t) \quad (5)$$

- where the distribution function of emitted protons

$$f(\vec{r}, \vec{p}, t) = g \left[ \exp\left(\frac{\gamma(E - \vec{p}\vec{v} - \mu) + T\delta}{T}\right) + 1 \right]^{-1} \quad (6)$$

- Here the spin factor  $g = 2$ ,  $E = \sqrt{p^2 + m^2}$ ,  $\gamma$  and  $\vec{p}$  are respectively the total energy, the Lorentz factor and the proton momentum;  $\vec{v}(\vec{r}, t)$  is the velocity field,  $G(b)$  is the factor taking into account that the cross section of the hot spot formation is always greater than the geometric one,  $\mu$  is the chemical potential, which is found from the conservation of the average number of particles for a grand canonical ensemble,  $T$  is the temperature,  $\delta$  is correction for the microcanonical distribution, which for the kinetic energy  $\varepsilon = E - m > E_1$  is equal to

$$\delta = \left[ -M \ln \left( 1 - \frac{\gamma(E - \vec{p}\vec{v}) - m}{MT} \right) - \frac{\gamma(E - \vec{p}\vec{v}) - m}{T} \right] \quad (7)$$

where  $M = 3N / 2$ ,  $N$  is the number of nucleons in the thermostat,  $E_1 (E_1 \gg T)$  is the energy that is close to the energy of the thermostat, i.e. close to the kinematic limit for the energy of the system. We also chose the energy value  $E_2 (E_2 < E_1)$ , when the distribution function decreases by an order of magnitude compared to its maximum. When  $\varepsilon < E_2$  the amendment  $\delta$  was supposed equal to zero. In the energy interval  $E_2 > \varepsilon > E_1$  it was a linear interpolation between zero and expression (7). Here the correction  $\delta$  is found for the Boltzmann limit of an ideal gas, since deviations from a grand canonical distribution of the Fermi gas are manifested on the "tails" of the energy spectra when the Fermi distribution coincides with the Boltzmann limit.

- The probability of a microcanonical distribution in the limit of the Boltzmann limit of an ideal gas is

- $$w(\vec{r}, \vec{p}) = C_M \left( 1 - \frac{\varepsilon}{U} \right)^M = C_M \exp \left( M \ln \left( 1 - \frac{\varepsilon}{MT} \right) \right) \quad , \quad (8)$$

- where  $\varepsilon$  is the kinetic energy of the system,  $U = MT$  is the energy of the thermostat,  $C_M$  is the normalization factor. As a result, in the limit of a large number of particles  $N$  at  $M = \frac{3}{2}N \rightarrow \infty$ , expression (8) becomes a grand canonical distribution

- $$w_0(\vec{r}, \vec{p}) = C_M \exp\left(-\frac{\varepsilon}{T}\right)$$

- Thus, on the tails of the energy distributions, using formula (7), we find an amendment for the microcanonical distribution (6), which changes the usual Fermi-Dirac distribution, describing the system well away from the tails of the proton spectrum. Moreover, in formulas (5) - (6) it is taken into account that the energy of the system is recalculated in accordance with the Lorentz transformations. The energy in the distribution (6) is reckoned from the value of the self-consistent mean field with allowance for the surface energy, since the nucleons are "locked" by the mean field.
- In addition to the contribution of (1) to the cross section for the emission of protons from the hot spot, we also took into account the contribution from the fusion of the non-overlapping parts of the colliding nuclei so called "spectators".

Fig.2.  $^{12}\text{C}+^9\text{Be}$  300MeV/nucl.  
(protons)  $3,5^0$

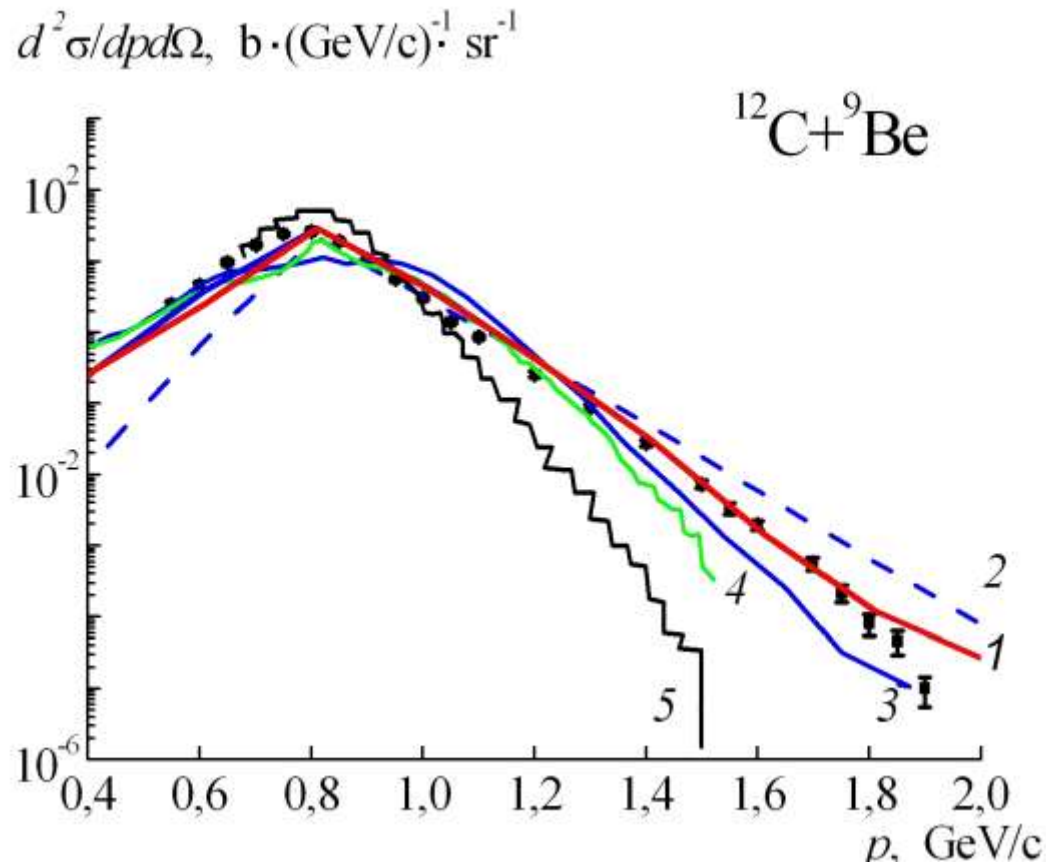


Fig.3.  $^{12}\text{C}+^9\text{Be}$  600 MeV/nucl.  
(protons)  $3,5^0$

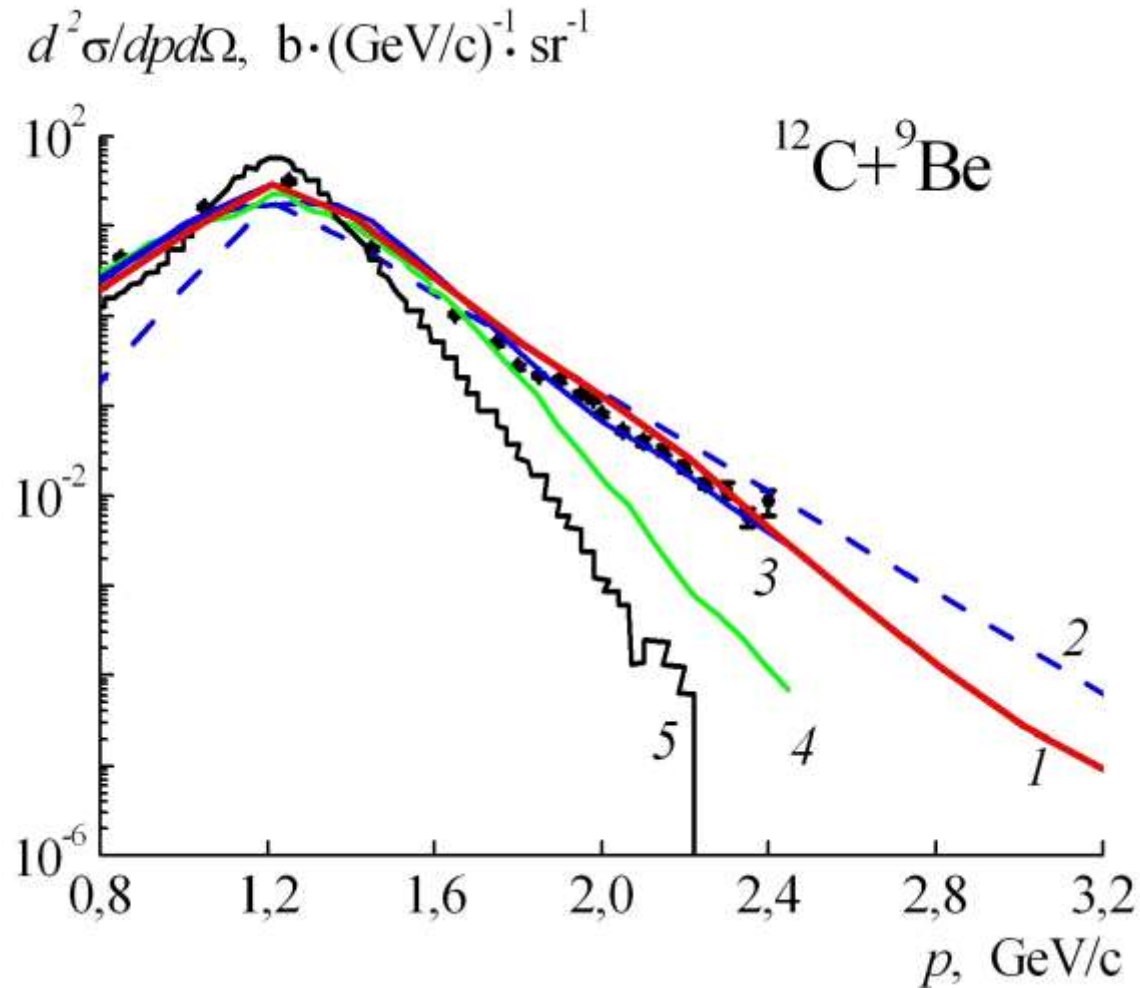


Fig.4.  $^{12}\text{C}+^9\text{Be}$  950 MeV/nucl.  
(protons)  $3,5^0$

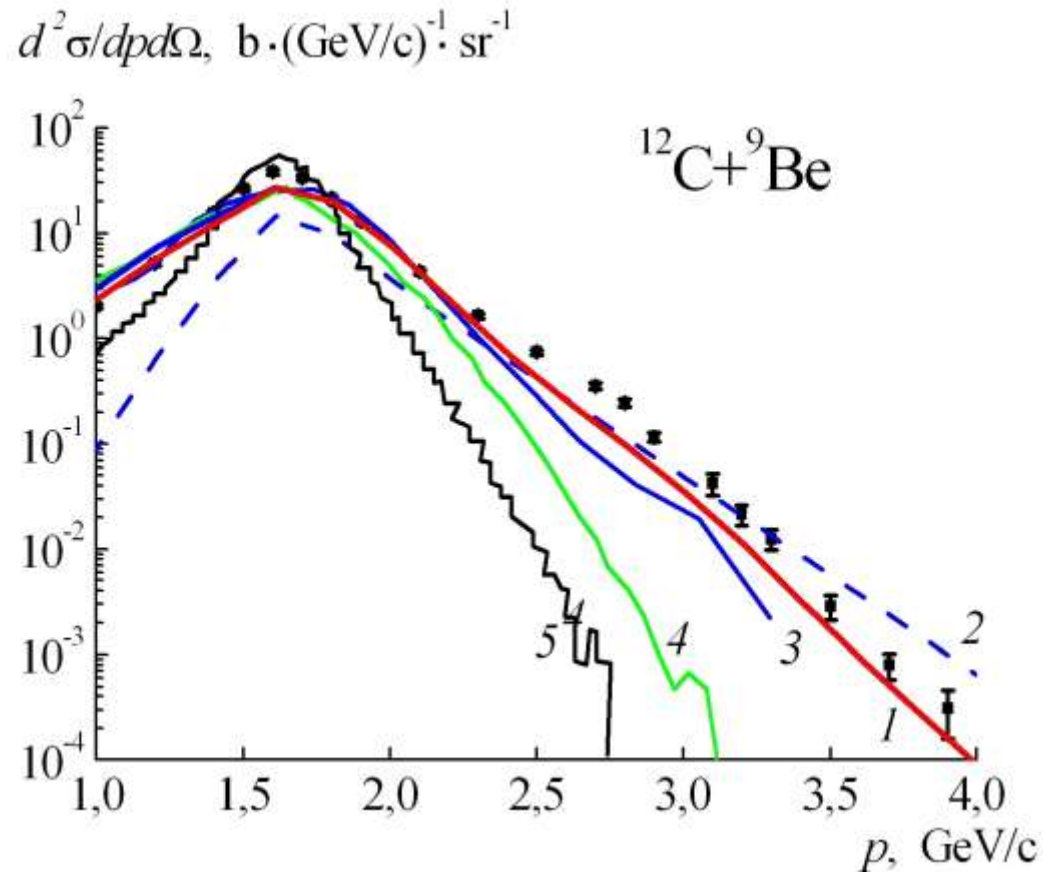
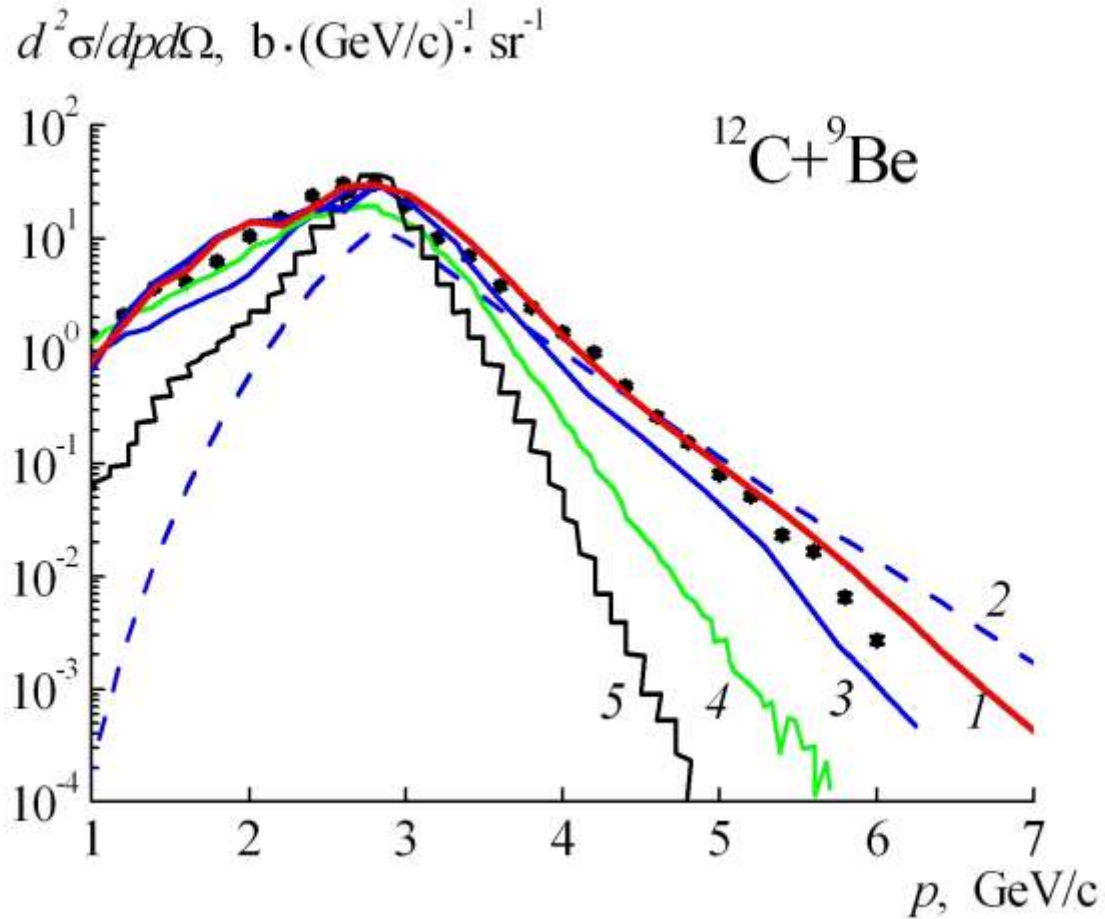


Fig.5.  $^{12}\text{C}+^9\text{Be}$  2 GeV/nucl.  
(protons)  $3,5^0$



# Fig. 6. $^{40}\text{Ar}+^{40}\text{Ca}$ 92 MeV/A (protons)

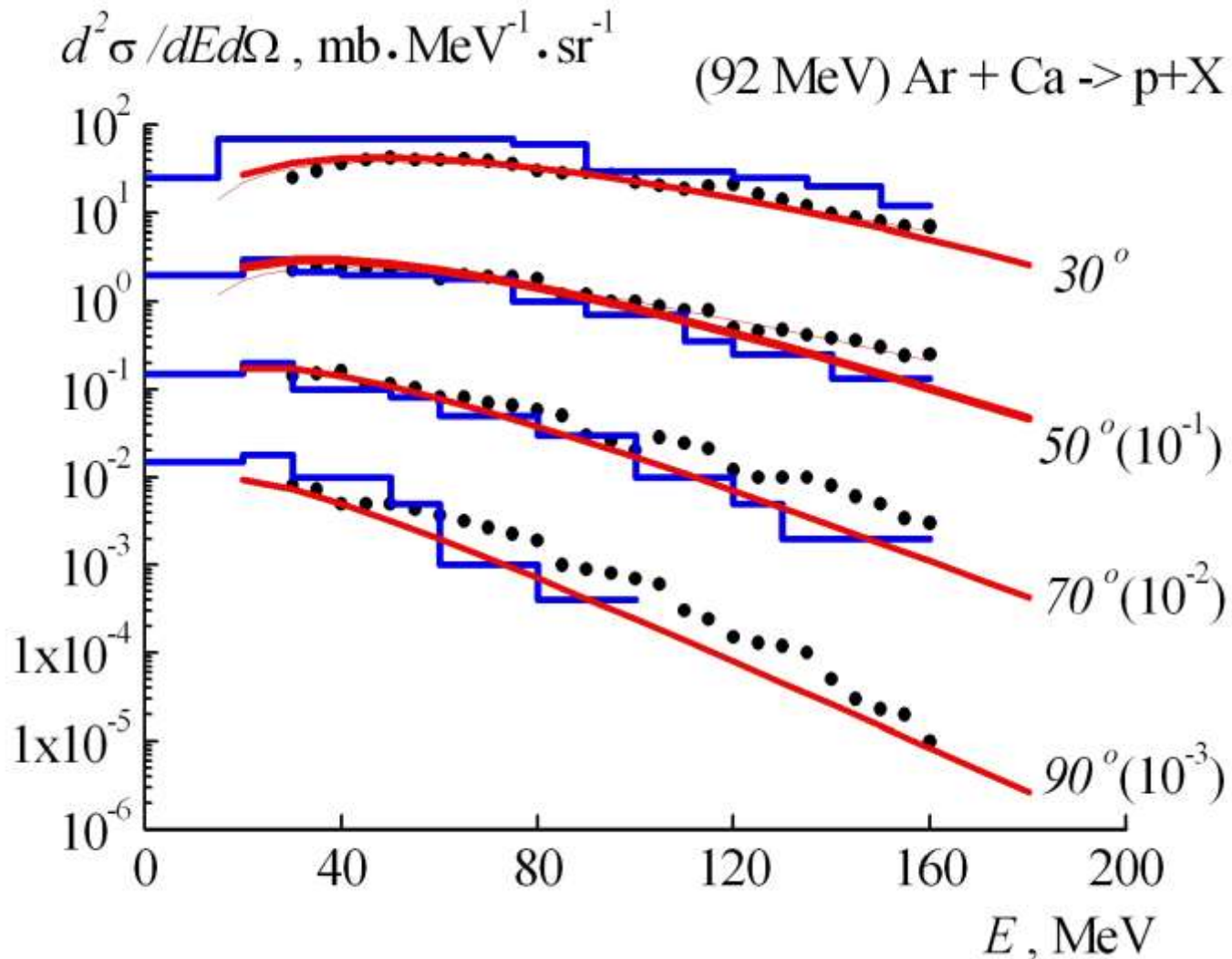




Fig.7.  $^{16}\text{O}$  94 MeV/A  $90^\circ$   
(subthreshold pions)

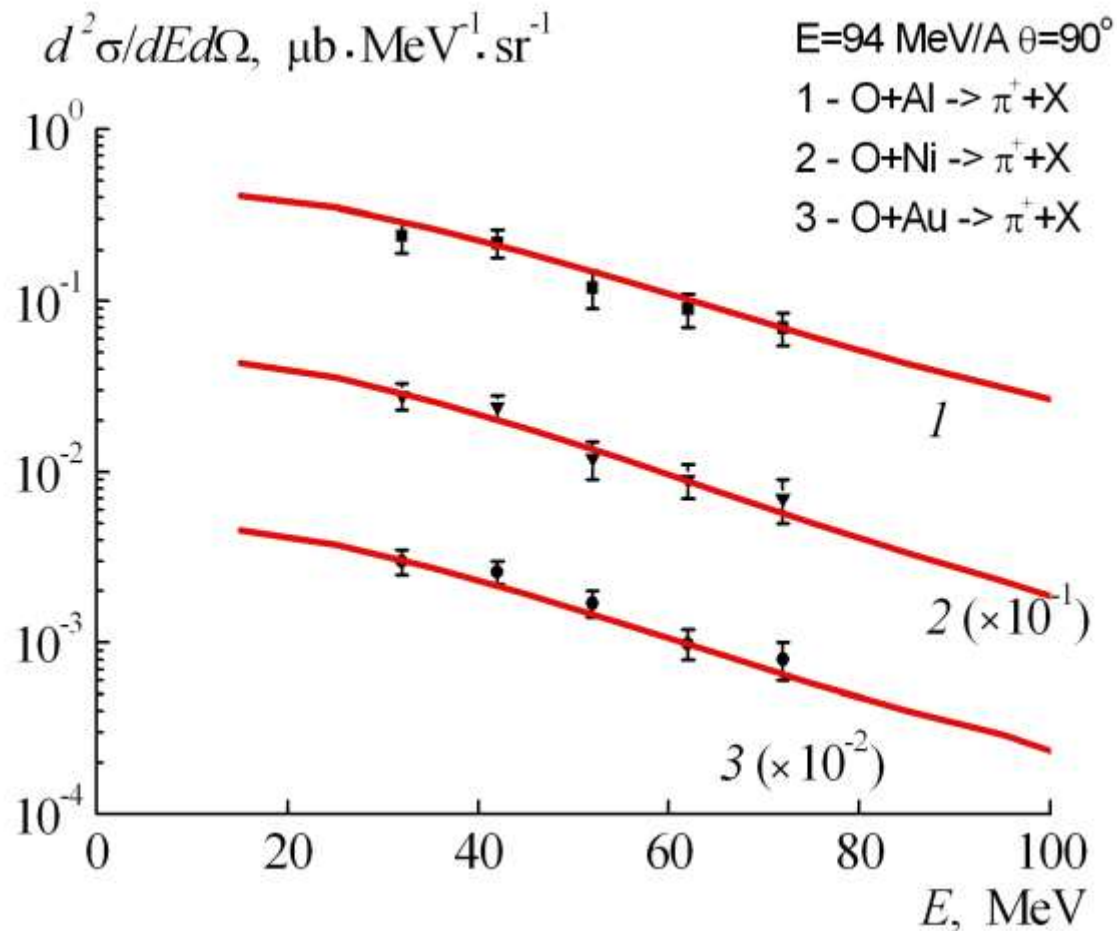
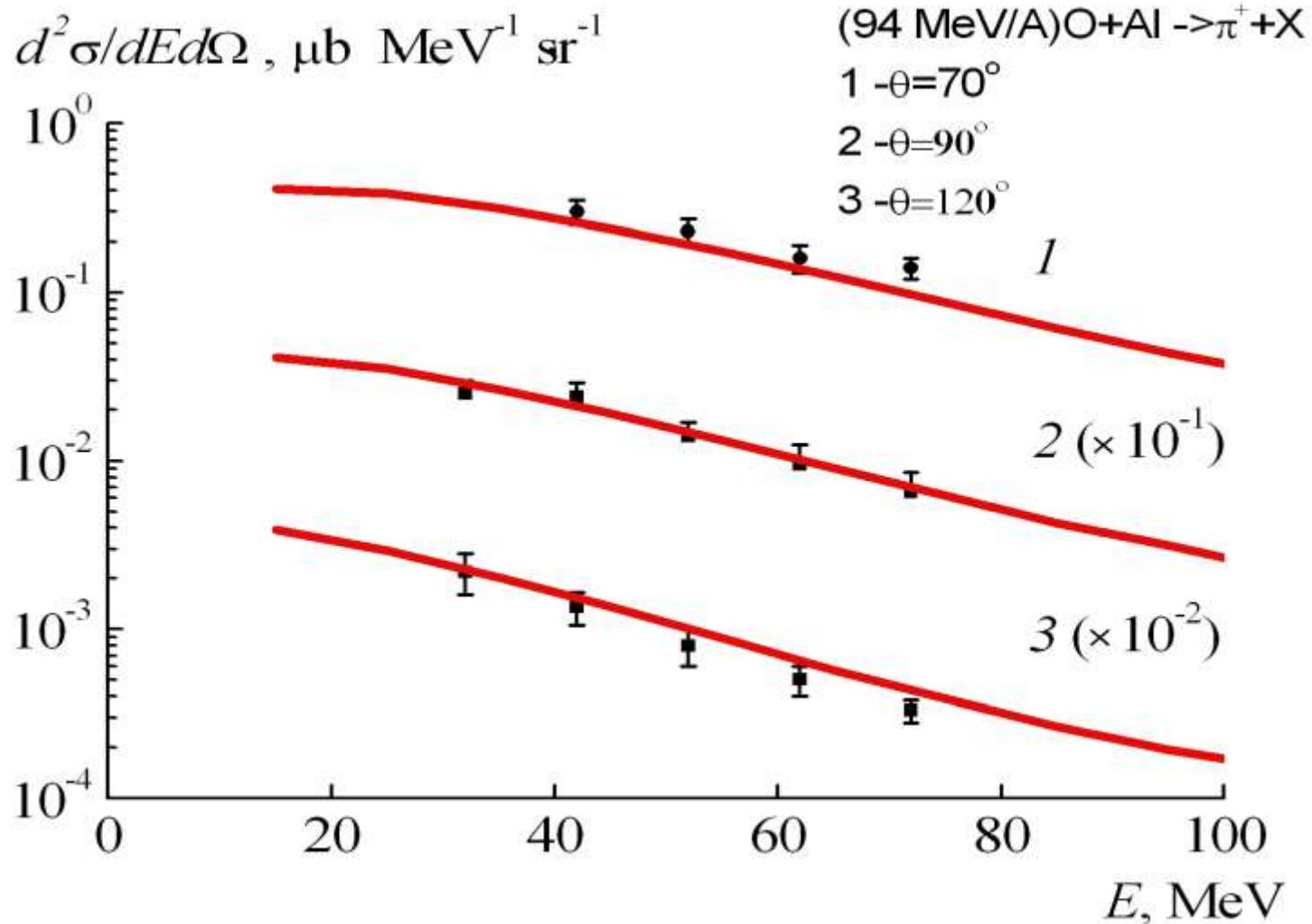


Fig. 8.  $^{16}\text{O}+^{27}\text{Al}$  94 MeV/A  
(subthreshold pions)



- In Fig. 2-5 are shown the momentum spectra of protons emitted in the  $^{12}\text{C}+^9\text{Be} \rightarrow \text{p}+\text{X}$  reaction at an angle of  $3.5^\circ$  at an  $^{12}\text{C}$  ion energy of 300 MeV / nucl., 600 MeV/nucl., 950MeV/nucl.and, 2GeV/nucl. The experimental data [20] are marked by points. The solid curve 1 is our calculation. The dashed curve 2 is our calculation without taking into account an amendment for the microcanonical distribution and without fragmentation. Curves 3, 4, 5 are results of calculations for transport codes [20]. Curve 3 corresponds to the cascade model [32], curve 4 corresponds to the transport model of quark-gluon strings [33], curve 5 corresponds to the quantum molecular dynamics (QMD) model built into the GEANT4 package [34]. As can be seen from this figures, in the cumulative region of the spectrum our calculation turned out to be in agreement with the experimental data [20]. The decline in the cross sections by 5 orders of magnitude is reproduced in our approach no worse than in the Monte Carlo transport codes. Some cascade calculations noticeably underestimate these experimental data in the high-momentum region. And in the region of small momentums, our calculation reproduce the experimental data too, which may be due to the contribution from the protons formed as a result of  $^{12}\text{C}$  fragmentation. An amendment for the microcanonical distribution (red curve 1 in contrast blue curve 2) appears in this case only at the very tails of the high-momentum distributions of the protons

- In order to make sure that our approach is applicable not only to the reactions described above, we present a description of other experimental data. For example, we also managed to reproduce the experimental data of the experiment from [6] on the energy spectra of protons and negative pions emitted in the reaction  $^{20}\text{Ne} + ^{208}\text{Pb} \rightarrow \text{p} (\pi^-) + \text{X}$  at a  $^{20}\text{Ne}$  nucleus energy of 2.1 GeV / nucleon (Fig. 9.10), and also in the reaction  $^{40}\text{Ar} + ^{40}\text{K} \rightarrow \text{p} + \text{X}$  at a nuclear energy of  $^{40}\text{Ar}$  equal to 1.8 GeV / nucleon [6] (Fig. 11).
- To describe the emission of pions, expressions (5) and (6) can be used, where function (6) can be used as the pion distribution function by setting the mass of pions to be equal everywhere 140 MeV, and the chemical potential equal to zero, since the number of pions is not specified, for negative pions, and 1 in expression (6) must be replaced by -1, since pions are bosons. In addition to thermal ones, the cross section for the production of  $\pi$ -mesons is also made by the decay channel  $\Delta \rightarrow N + \pi^-$ , which we included in the consideration similarly to [6]. In calculating the proton yields, the contribution from fragmentation in the regions of both overlapping and non-overlapping regions of colliding nuclei was taken into account.
- The reactions considered are of interest for experiments carried out at the SIS / GSI accelerator (Germany) and can be transferred to the energy range of the NICA accelerator complex under construction at JINR (Dubna).

Fig. 9.  $^{20}\text{Ne}+^{208}\text{Pb}$  2.1 GeV/A  
(protons)

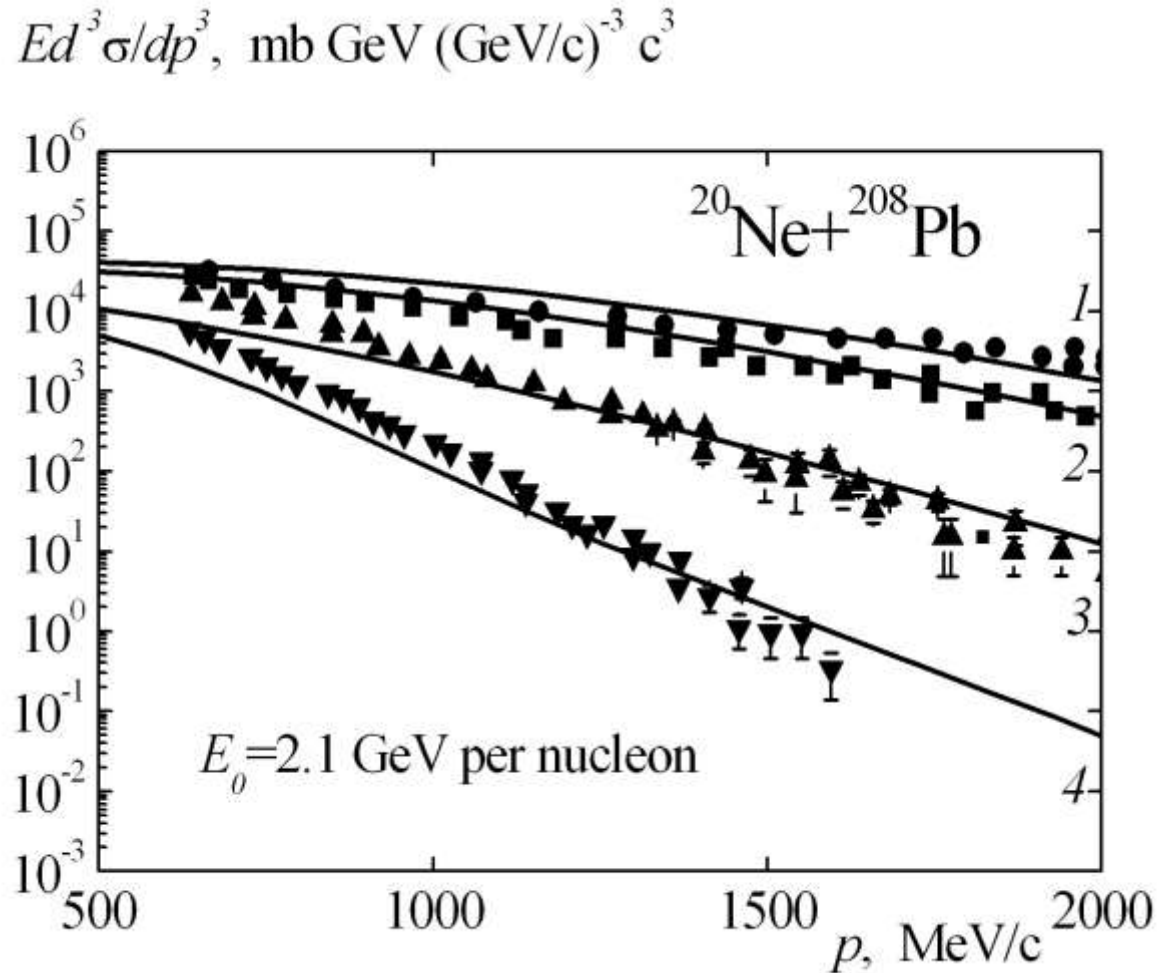


Fig. 10.  $^{20}\text{Ne}+^{208}\text{Pb}$  2.1 GeV/A  
(negative pions)

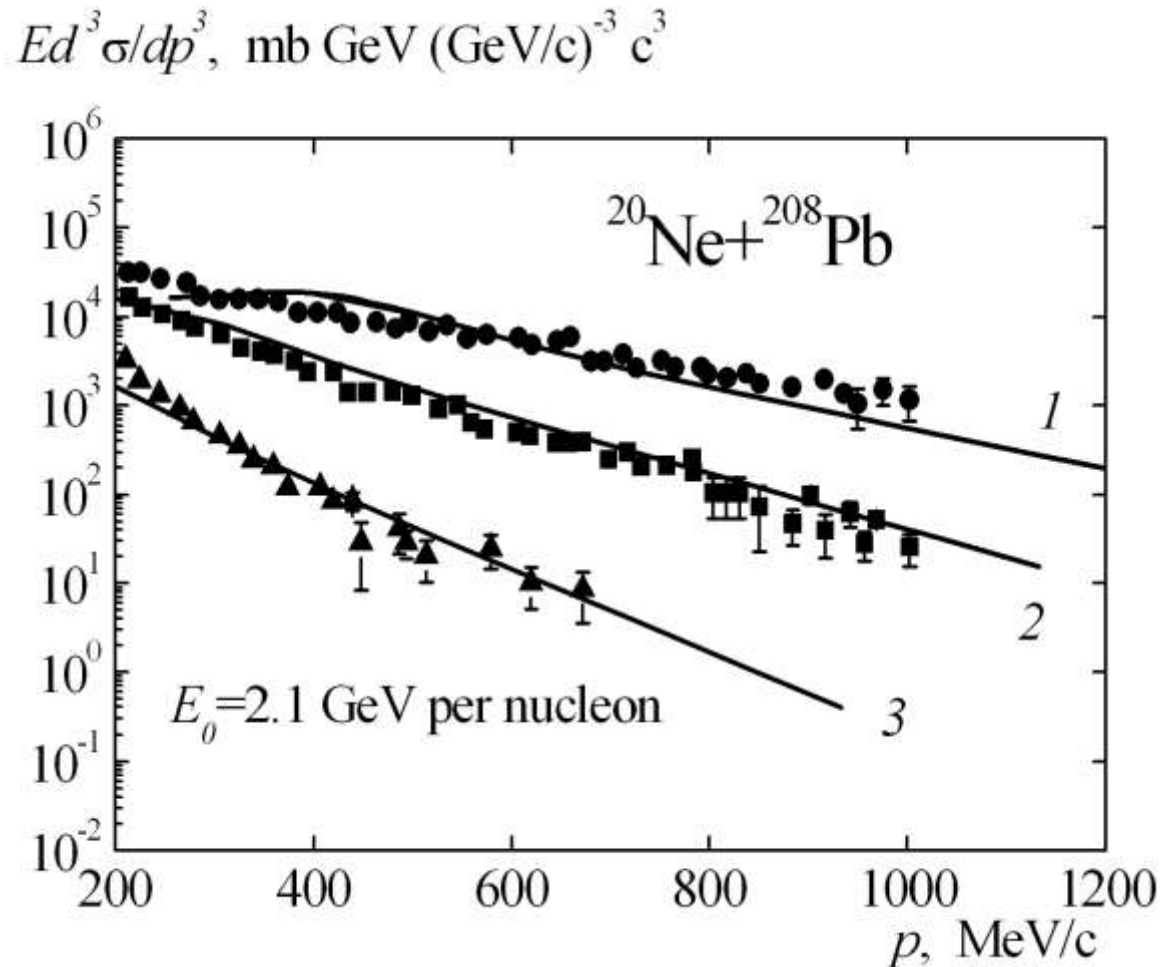
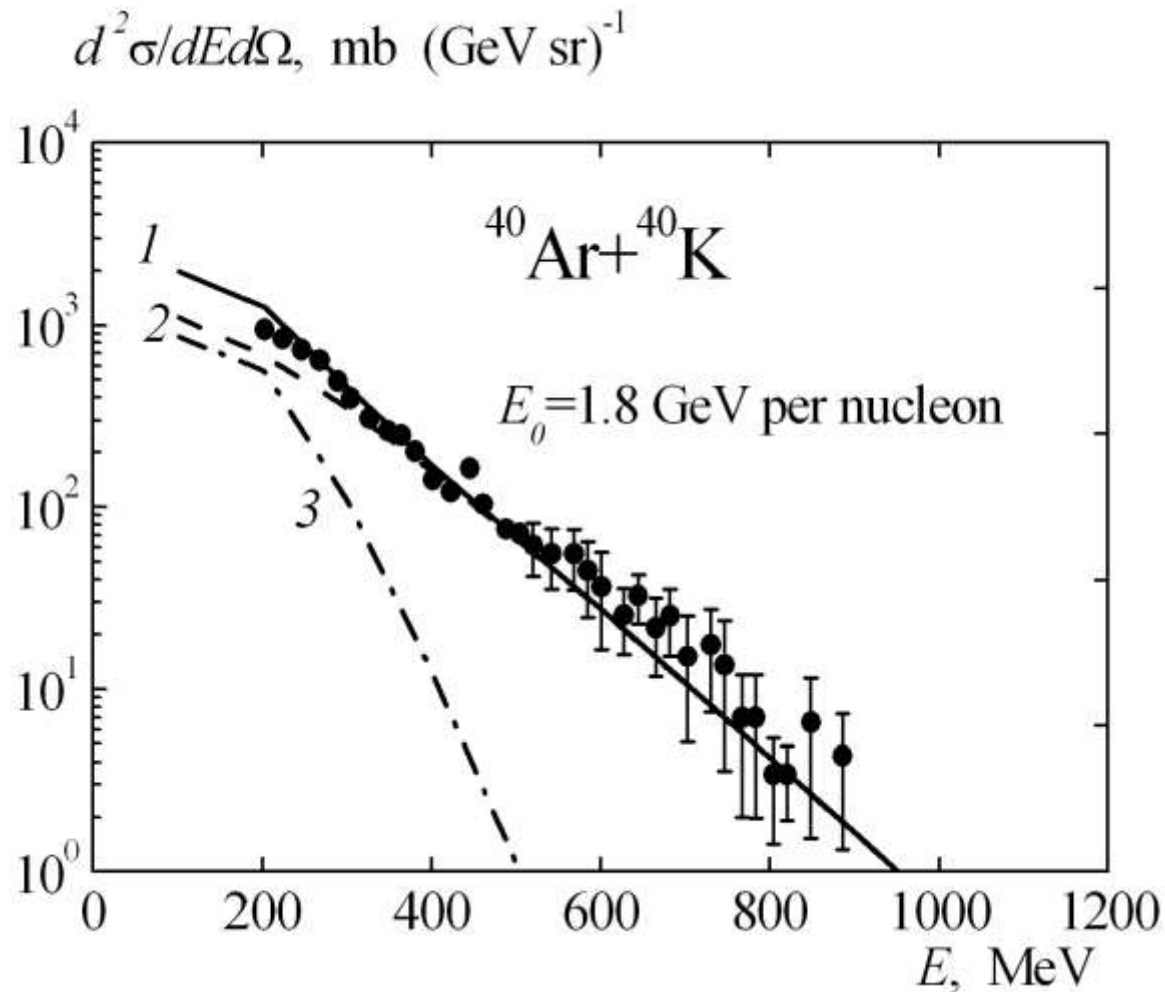


Fig. 11.  $^{40}\text{Ar}+^{40}\text{K}$  1.8 GeV/A  
(negative pions)



# Conclusion

- Thus, in this paper, the idea of using of a non-equilibrium equation of state in the hydrodynamic approach to describe the high-momentum proton and pion spectra emitted in heavy-ion collisions over a wide energy range has been further developed. We also succeeded in the description of the subthreshold pion energy spectra.
- The experimental shoulder in the cross section for the production of protons in the cumulative region is reproduced by our calculations, and sometimes by cascade models. The cumulative gamma-quanta is reproduced by ours too. Perhaps this may be due to the contribution of the rescattering of pions to the cumulative production of protons, considered earlier in [35].



# References

- 1. H. Stöcker and W. Greiner, Phys. Rep. **137**, 277 (1986).
- 2. A.S Khvorostukhin and V.D. Toneev, Phys. Atom. Nucl. **80**, 285 (2017).
- 3. A.S Khvorostukhin and V.D. Toneev, Phys. Part. Nucl. Lett. **14**, 9 (2017).
- 4. H Petersen, J. Steinheimer, G. Burau, M. Bleicher, and H. Stöcker, Phys. Rev. **C78**, 044901 (2008).
- 5. A.V. Merdeev, L.M. Satarov, and I.N. Mishustin, Phys. Rev. **C84**, 014907 (2011).
- 6. I.N. Mishustin, V.N. Russkikh, and L.M. Satarov, Sov. J. Nucl. Phys. **54**, 260 (1991).
- 7. Yu.B. Ivanov, V.N. Russkikh, and V.D. Toneev, Phys. Rev. **C73**, 044904 (2006).
- 8. A.T. D'yachenko and I.A. Mitropolsky, Phys. Atom. Nucl. **83**, 558 (2020).
- 9. A.T. D'yachenko and I.A. Mitropolsky, Bull. Russ. Acad. Sci. Phys. **84**, 391 (2020).
- 10. A.T. D'yachenko and I.A. Mitropolsky, EPJ Web of Conf. **204**, 03018 (2019).
- 11. A.T. D'yachenko and I.A. Mitropolsky, Phys. Atom. Nucl. **82**, 1641 (2019).
- 12. A.T. D'yachenko and I.A. Mitropolsky, Bull. Russ. Acad. Sci. Phys. **80**, 916 (2016).
- 13. A.T. D'yachenko and I.A. Mitropolsky, Bull. Russ. Acad. Sci. Phys. **81**, 1521 (2017).
- 14. A.T. D'yachenko, K.A. Gridnev, W. Greiner, J. Phys. **G40**, 085101 (2013).
- 15. A.T. D'yachenko, Phys. Atom. Nucl. **57**, 1930 (1994)..
- 16. P. Bonche, S. Koonin, J.W. Negele, Phys. Rev. **C13**, 1226 (1976).
- 17. G. D. Westfall *et al.*, Phys. Rev. Lett. **37**, 1202 (1976).
- 18. K.K. Gudima and V.D. Toneev, Sov. J. Nucl. Phys. **42**, 409 (1985)..
- 20. B.M. Abramov *et al.*, Phys. Atom. Nucl. **78**, 373 (2015).
- 21. K. Urmosy, G.G. Barnafoldi, and T.S. Biro, Phys. Lett. **B718**, 125 (2012).
- 22. C. Bignamini, F. Becattini, and F. Piccelini, arXiv:1204.2300v1(2012).
- 23. C.Y. Wong and G. Wilk, Phys. Rev. **D87**, 114007 (2013).
- 24. A.S. Goldhaber, Phys. Lett. **B53**, 306 (1974).
- 25. H. Feshbah and K. Huang, Phys. Lett. **B47**, 300 (1973)..
- 26. G. Bertsch, Z. Phys., **A289**, 103 (1978).
- 27. V.M. Kolomietz and H.H.K. Tang, Physica Scripta. **24**, 915 (1981).
- 28. C.Y. Wong and J.A. McDonald, Phys. Rev. **C16**, 1196 (1977).
- 29. K. Huang, *Statistical Mechanics* (Wiley, New York, 1987).
- 30. L. D. Landau and E. M. Lifshitz, *Course of Theoretical Physics*, Vol. 5: *Statistical Physics* (Pergamon, Oxford, 1980; Nauka, Moscow, 1976).
- 31. A. I. Anselm, Fundamentals of Statistical Physics and Thermodynamics (Nauka, Moscow, 1973) [in Russian].
- 32. A.V. Dementev and N.M. Sobolevsky, Nucl. Tracks Radiat. Meas. **30**, 553 (1999).
- 33. S.G. Mashnik *et al.*, LA-UR-08-2931 (Los Alamos 2008); arXiv.0805.0751[nucl-th].
- 34. T. Koi. *et al.*, AIP Conf. Proc. **896**, 21 (2007).
- 35. M.A. Braun and V.V. Vechernin, [Sov. J. Nucl. Phys. **43**, 1016 (1986)].

THANK YOU FOR ATTENTION!